# New Fabry-Perot Interferometers at McMurdo and South Pole Stations

Riley Troyer[1], Mark Conde[1], Don Hampton[1], William Bristow[1], Michael Kosch[2], Theo Davies[3], Mamoru Ishii[4]

1: Geophysical Institute University of Alaska, 2: South African National Space Agency; 3: La Trobe University; 4: NICT, Japan.

## Introduction:

In December 2015 and January 2016 the University of Alaska and partners installed two new all-sky imaging Fabry-Perot interferometers in Antarctica at McMurdo and South Pole stations. The instruments record Doppler spectra of airglow and auroral emissions from atomic oxygen in Earth's thermosphere, from which we can determine wind speed and temperature in the emission region. Both sites are located at similar magnetic latitudes (80S vs. 74S) but significantly different geographic latitudes (78S vs. 90S). Both are typically located near the equator-ward edge of the polar cap during quiet and moderate geomagnetic conditions.

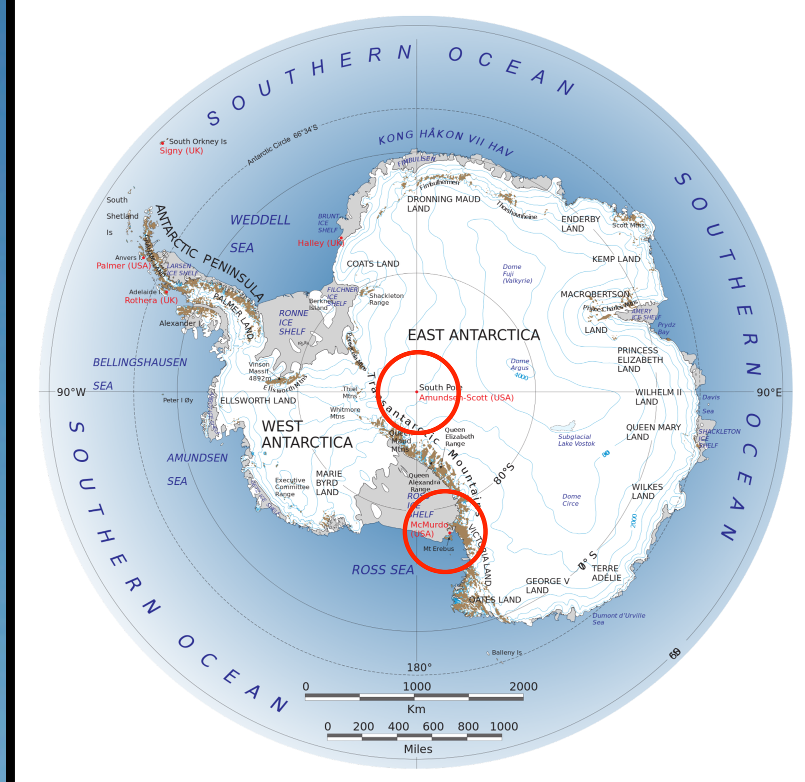


## Installation:

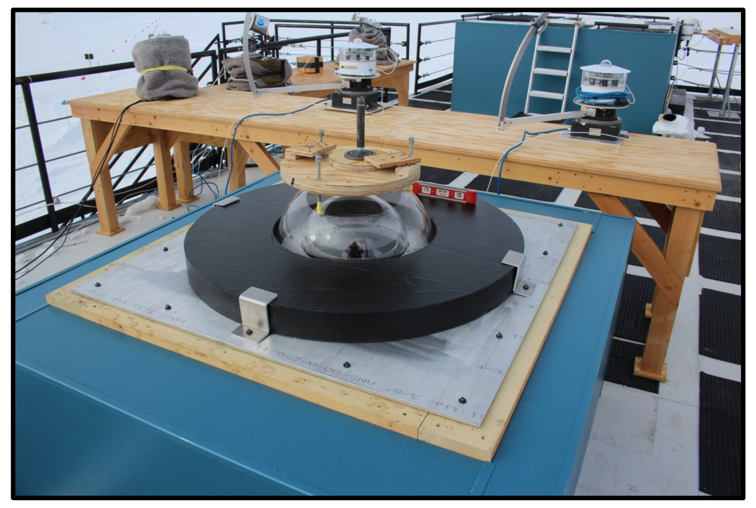

Figure 1: The primary all sky lens of the instrument must be enclosed within a double glass dome filled with nitrogen and surrounded by an insulating sheath to stop condensation of water in the extreme subzero temperatures. Photo taken by Dale Pomraning

Figure 2: The interferometers stand up to 5 meters tall when fully assembled. Photo taken by Dale Pomraning

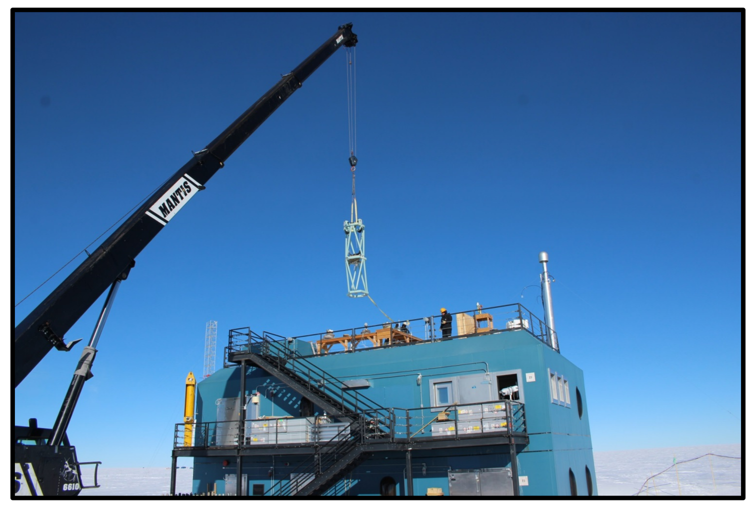

Figure 3: A large crane was used during installation of the mounting frame for the instrument at South Pole. Photo taken by Dale Pomraning

## Instrument:

1. Light is collected from the night sky with an all sky lens.
2. A narrow passband interference filter rejects all light apart from the emission line of interest (either 558 nm or 630 nm.)
3. The light then passes through a high-resolution Fabry-Perot etalon, comprised of two partially reflective (*R* around 0.85) parallel optical flats (polished to ~λ/100 flatness).
4. A high-quality telephoto lens forms Fabry-Perot fringes, from which we can derive spectra with an instrumental passband width of less than one picometer.
5. Wind speeds are then estimated from Doppler shifts of the emission line, whereas temperatures are derived from spectral widths.

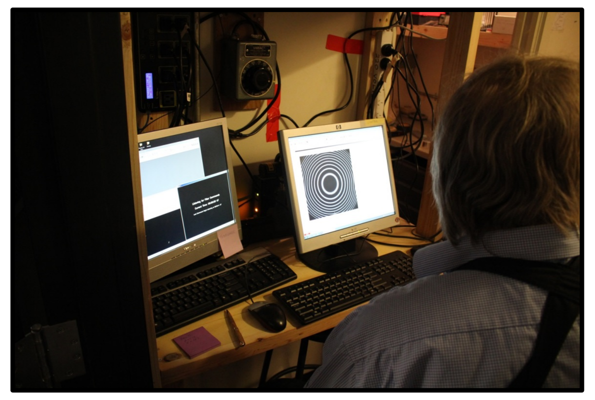

Figure 4: Circular Fabry-Perot fringes seen by the South Pole instrument. Doppler spectra are derived using computer processing of fringes recorded as the etalon gap is scanned over one order of interference. Photo taken by Dale Pomraning

Figure 5: Close up of the main optical assembly of the South Pole instrument. This view shows the etalon chamber, the (rare and expensive) Nikkor 300 mm f/2 fringe forming lens, and the Andor EMCCD camera. Photo taken by Dale Pomraning

## Wind Speed Data:

### South Pole Station

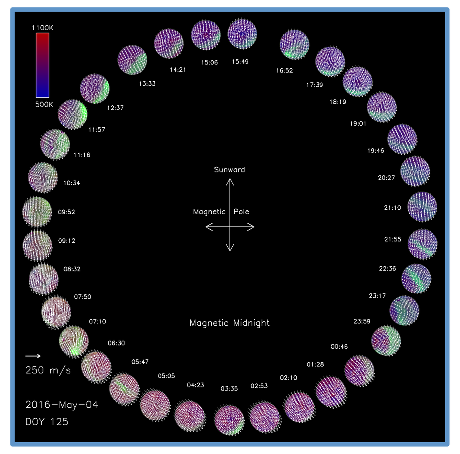


Figure 6: F-region wind velocity maps from the South Pole Station taken on May 4th 2016.

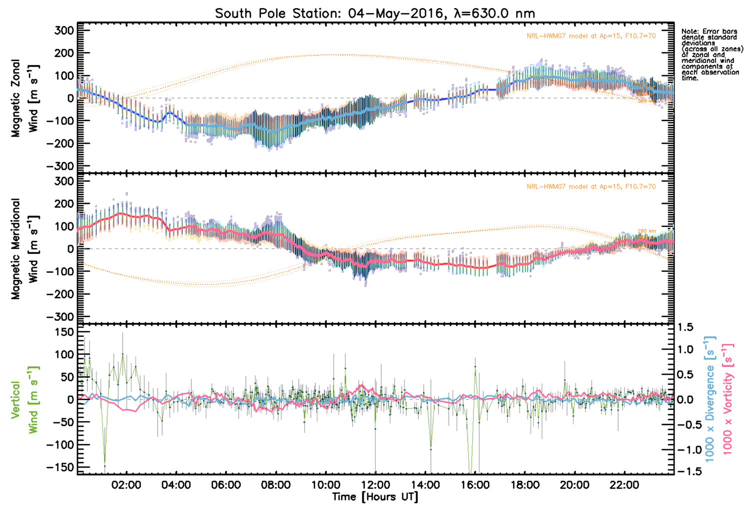


Figure 7: F-region components measured from South Pole Station taken on May 4th 2016.

### McMurdo Station

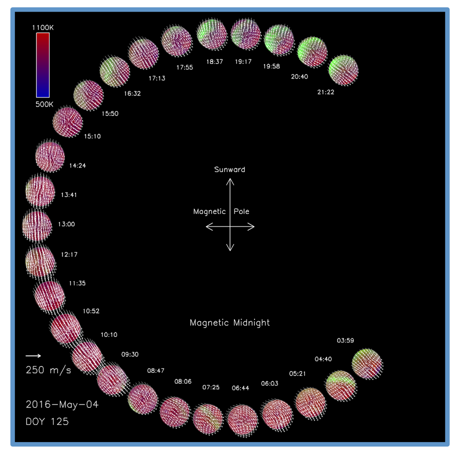


Figure 8: F-region wind velocity maps taken at the McMurdo Station on May 4th 2016.

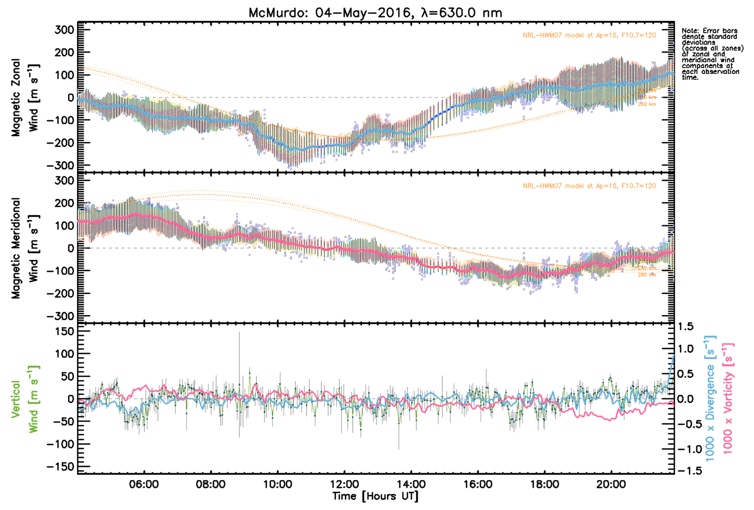


Figure 9: F-region wind components measured from McMurdo Station on May 4th 2016.

- These "all-sky" instruments view the sky in a zenith-centered circular field of view that extends down to about 70° zenith angle. Software divides this into (typically) 115 "zones", and an independent spectrum is derived for each zone.
- Numerical fitting is used to estimate the Doppler shift and spectral width for each zone. The distribution of Doppler shifts across the sky then allows us to infer the wind field.
- Figure 6 and figure 8 depict winds in a coordinate system such that the sunward direction is always oriented up the page. Winds at these latitudes are predicted to typically blow antisunward – and we do see this in our data. However we also signatures of local non-uniformity of the flow, and of wave perturbations.
- Figures 7 and 9 depict time series of individual wind components, together with estimates of divergence and vorticity.
- Our example day (May 4) was relatively quiet at both sites.

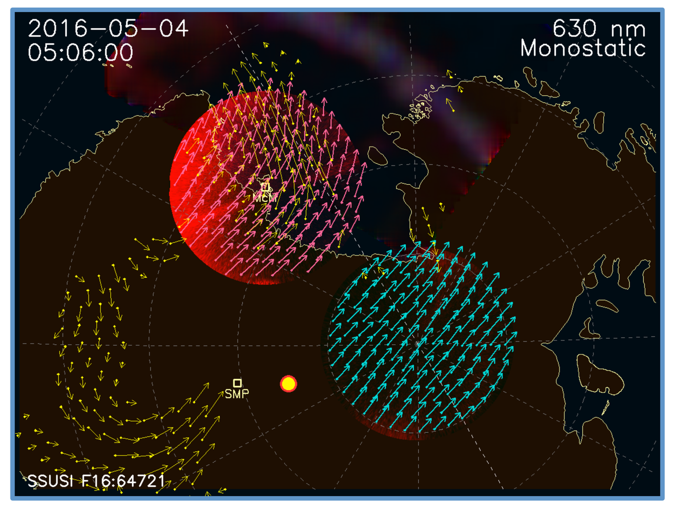


Figure 10: F-region wind vector maps for both McMurdo and South Pole stations on May 4th at 6:32 AM. Overlaid are auroral images from SSUSI instruments as well as ion vector maps. The yellow dot indicates the longitude of the sub-solar point.

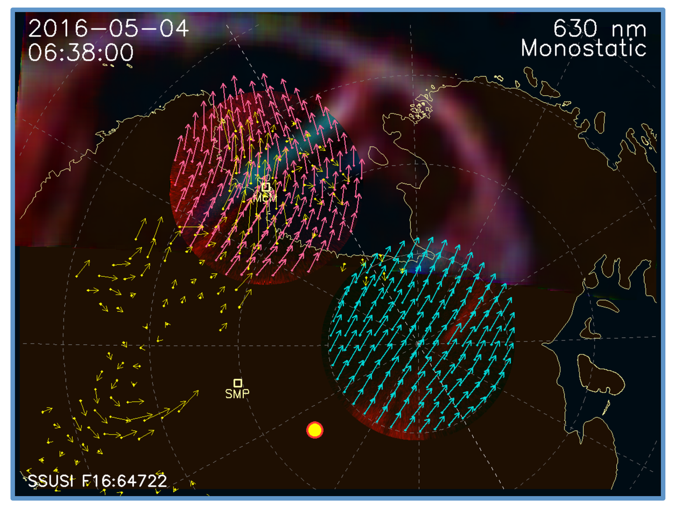


Figure 11: F-region wind vector maps for both McMurdo and South Pole stations on May 4th at 10:26 AM. Overlaid are auroral images from SSUSI instruments as well as ion vector maps. The yellow dot indicates the longitude of the sub-solar point.

## Temperature Data:

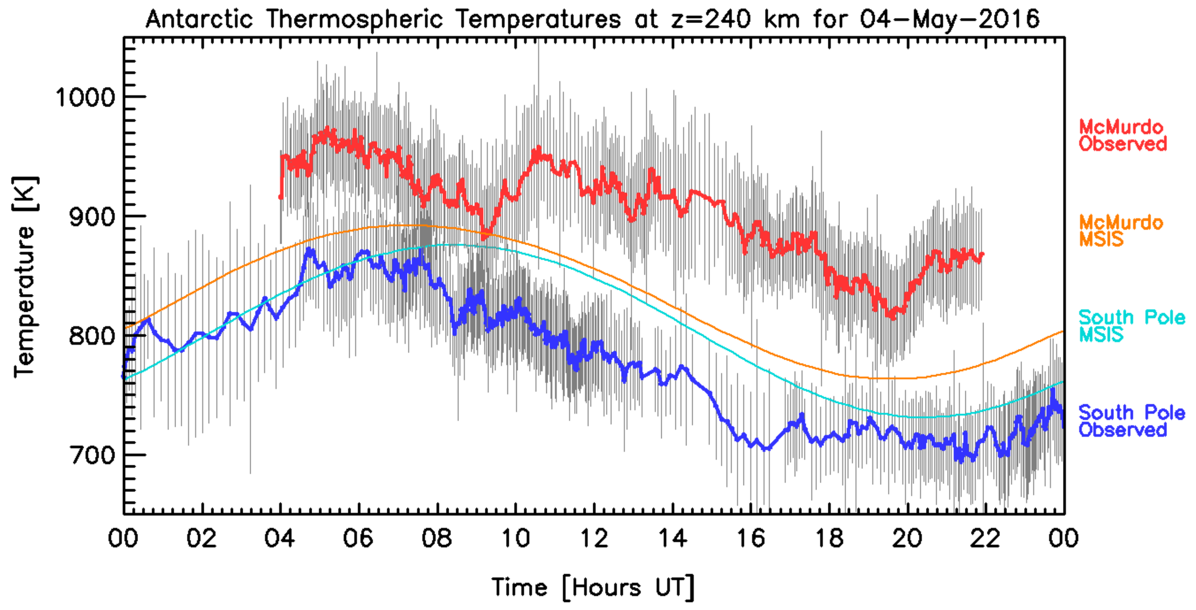


Figure 12: F-region atmospheric temperatures over May 4th 2016 taken at McMurdo and South Pole Stations along with predicted values from the MSIS atmospheric model.

- Kinetic temperatures in the emission region are estimated from spectral widths. However, the recorded spectra are (inevitably) slightly broadened by the non-zero passband width of the spectrometer itself, which means that accurate temperature estimates must take account of instrumental broadening.
- Currently, temperatures estimated from the instrument at McMurdo station are about 150K higher than the corresponding South Pole temperatures, and also higher than predicted by the MSIS model. This discrepancy appears unlikely to be physical. We suspect it is most likely due to a calibration issue, and we are investigating further.
- By contrast, temperatures from South Pole are not substantially different to predictions from MSIS.

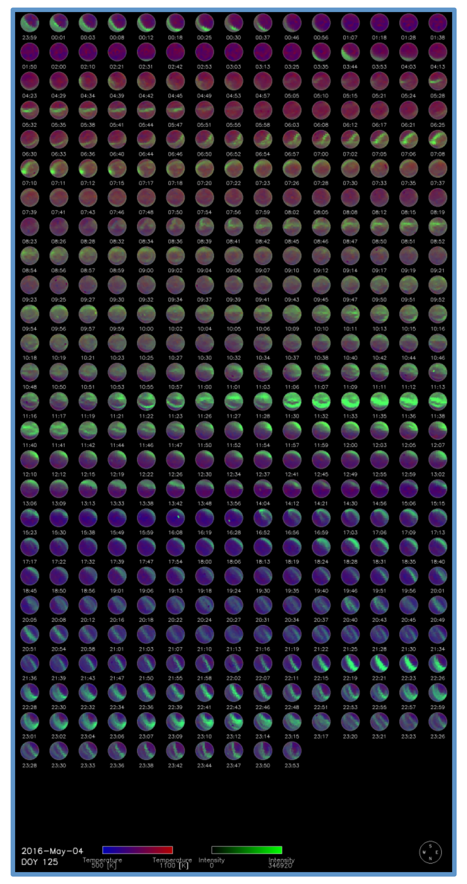


Figure 13: F-region temperature skymaps overlaid with 630 nm intensity taken from South Pole Station on May 4th 2016 .

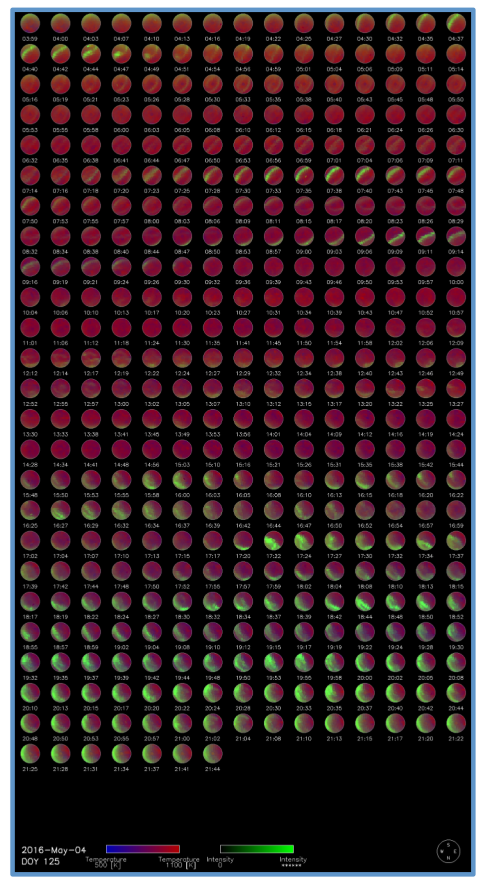


Figure 14: F-region temperature skymaps overlaid with 630 nm intensity taken from McMurdo Station on May 4th 2016 .

Background image taken by Dale Pomraning